Proceedings of IMECE'03
2003 ASME International Mechanical Engineering Congress & Exposition
Washington, D.C., November 16-21, 2003

IMECE2003-41912

NUMERICAL STUDY OF MIXING IN MICROCHANNELS WITH PATTERNED ZETA POTENTIAL SURFACES

Seungbae Hong
Department of Mechanical Engineering
Columbia University, New York, NY 10027

Jean-Luc Thiffeault
Department of Mathematics
Imperial College London, United Kingdom

Luc Fréchette
Department of Mechanical Engineering
Columbia University, New York, NY 10027

Vijay Modi
Department of Mechanical Engineering
Columbia University, New York, NY 10027

ABSTRACT

In a recent study, an effective means of mixing a low Reynolds number pressure-driven flow in a micro-channel was reported by Stroock et al.[10] using trenches on the lower wall that form a staggered herringbone pattern. In the present work numerical results are reported that indicate enhanced mixing using a similar herringbone pattern in the context of an electro-osmotically driven flow in microchannels. Instead of trenches, all walls are flush, making microfabrication easier. The lower wall would have lithographically deposited polymer coatings that exhibit a zeta potential of a sign opposite to that at the other walls. These coatings are chosen to form a herringbone pattern.

If mixing can be achieved using purely electro-osmotic flows, then it becomes easier to scale the channel dimensions to smaller values without the penalty of a dramatic increase in pressure drop. Moreover, the possibility of mixing with purely electro-osmotic flows that do not require time varying electric fields leads to a simpler system with fewer moving parts. With current micro-fabrication techniques, it is difficult to produce periodic patterned coatings on all four walls of a rectangular microchannel. For this reason, this study limits its scope to coatings applied only on the lower surface of the microchannel, with a rectangular cross-section.

Numerical simulations are used in order to elucidate the dominant mechanism responsible for mixing, which is identified as the blinking-vortex [3]. The flow regime chosen to illustrate these effects is the same as that used by Stroock et al.[10], characterized by Reynolds numbers that are $O(10^{-2})$ and Péclet numbers that are of $O(10^{5})$. The presence of patterned zeta potentials in a microchannel violates conditions of ideal electro-osmosis [4] and hence the flows are necessarily three-dimensional.

The efficiency of mixing is quantified by examining particle tracks at several downstream sections of the microchannel and averaging their concentration over boxes of finite size to model diffusion. It is found that the standard deviation of the concentration decays exponentially, and that the rate of decay is independent of the Péclet number when the latter is sufficiently large, indicating that chaotically-enhanced mixing is occurring.

INTRODUCTION

Mixing is difficult in many microfluidics applications because the flow regime is usually laminar, inertia effects are weak, and frequently the diffusion coefficients of the species of interest are low. In a laminar uniaxial flow, mixing is purely diffusive. The typical microchannel cross-section dimensions and average velocities are respectively of the order of 1 mm and 100 μm/sec. The diffusion coefficient (D_{AB}) for large molecules such as DNA and proteins in water is about 5×10^{-12} m^2/sec. The resulting Reynolds number is less than unity (Re ≈ 0.01–0.1), and the Péclet number ($Pe = U{\cdot}w/D_{AB} \approx 20{,}000$, where U is the average flow speed and w is the characteristic cross-section width) is very large, requiring long mixing time if driven only by diffusion. The characteristic axial distance for diffusive mixing (where the diffusion distance is roughly the channel width) is $l \approx w \times Pe \approx 20$ m. The resulting channel length for diffusive mixing in this regime can be prohibitively long. An enhanced mixing time can benefit applications such as DNA and protein analysis, cytometric analysis, flow injection, and chemical synthesis reactors.

Researchers have proposed a variety of mixing mechanisms for low Reynolds numbers laminar flows, with those utilizing chaotic phenomena being relatively easy to fabricate. Active chaotic mixers require an external power

source to utilize electrokinetic instability [9], external pressure perturbation [7], magnetic beads [12], and polystyrene particles [5] to achieve rapid mixing. Passive chaotic mixers use geometric features instead of external power source to enhance mixing. Notable studies have exploited serpentine channels [8], staggered herringbone patterns for pressure driven flow [10], and well structures in the trapezoidal channel cross-section for electro-osmotic flow [6].

In this paper, a novel passive mixer is introduced that uses a periodic zeta potential coating to induce chaotic fluid flow in electro-osmotically driven microfluidic devices. Using periodic zeta potential coatings on a flush surface, we can induce vortices in the creeping flow regime. The mixer performance is tested using particle orbit information. A simple particle-dispersion method is used to estimate the standard deviation (a measure of the deviation of the concentration field from the mean), which allows a characterization of the efficiency of mixing.

DEVICE DESCRIPTION

We first examine a simple mixer concept in order to understand the nature of fluid flows with patterned surfaces. Figure 1 shows a schematic diagram of a microchannel mixer configuration. The mixer consists of a straight channel with a rectangular cross-section and periodic zeta potential patterning on the bottom surface. With the application of an external electric field along the channel length, the resulting three-dimensional fluid flow can be very complex, depending on the zeta potential strength combinations and the pattern geometry. To help understand the complex flow field resulting from a specific pattern, we begin with patterns consisting of simple stripes with an angle as shown in Figure 2 (a) and later examine more complex flow resulting from herringbone patterns shown in Figure 2 (b).

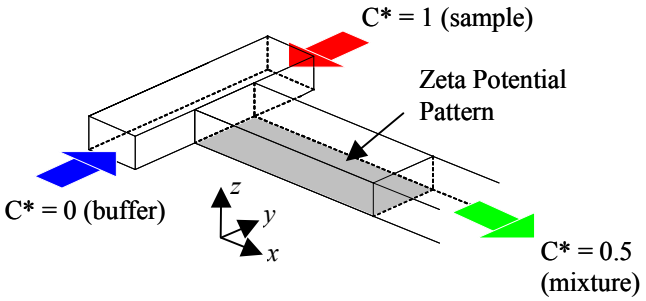

Figure 1: Micromixer configuration

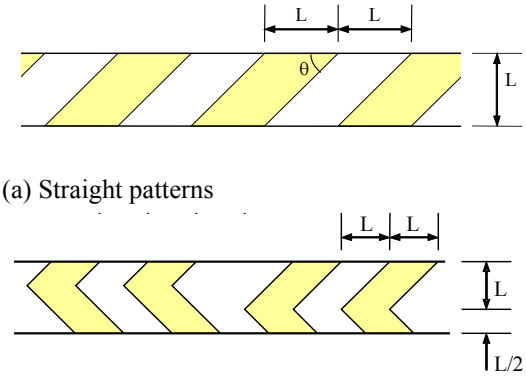

Figure 2: Channel and Pattern Shapes (top view)

In the pattern shown in Figure 2 the channel bottom surface (including the other three sides of the wall) is assumed to have a zeta potential of , while the shaded patterns have a zeta potential of , which is the same in magnitude but in the opposite direction to the induced electro-osmotic flow. The resulting flow is predominantly influenced by the electro-osmotic flow, while the pattern provides a perturbation that assists the mixing mechanism. Above the patterns, vortices form as shown in Figure 3. There are experimental [11] and analytical [1] studies on the existence of such vortices in a microchannel when two adjoining surfaces possess opposite zeta potentials.

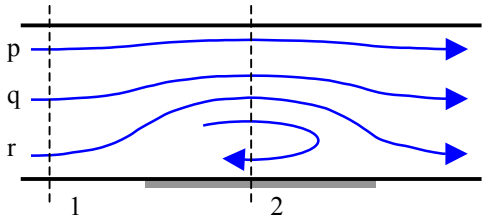

Figure 3: Flow patterns (*y* plane view)

If the pattern is rectangular, i.e. $\theta = 90°$ in Figure 2 (a), the vortex is aligned normal to the flow direction, thus there is no velocity component in the *y*-direction (see Figure 1 for the axis directions). Such a flow field is of little use for mixing fluids. But as θ deviates from 90° and gets close to 45° the y-velocity component becomes larger. Since the flow is moving in a confined channel, to satisfy continuity there is an opposite *y*-velocity component, and together these result in another vortex in the channel. This secondary vortex is useful for mixing since its direction is along the fluid flow.

We now examine the vortex motion in more detail by following hypothetical particles in the flow. The path lines in Figure 3 track three different particles, p, q, and r, introduced upstream (left hand side of the channel). These represent a considerably simplified view of the actual behavior. The secondary vortex is primarily in the bottom half of the channel. The motion of the particles that are labeled q and r in Figure 3, located at the center and bottom of the channel, is summarized in Figure 4. This vortical motion is critical to the use of a "blinking-vortex" model of the flow, to be examined later.

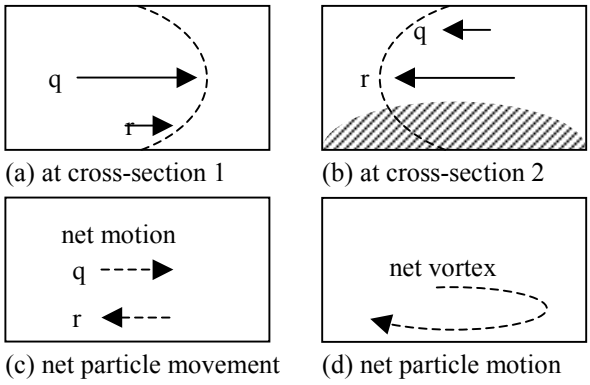

Figure 4: Flow patterns (*x* plane view). Shaded area in (b) represents re-circulation region where *x*-velocity is negative.

At the channel wall, regardless of patterning, the velocity in the x, y, z directions are respectively ±1, 0, and 0. Therefore, the y-velocity component has no-slip boundary conditions at the top and bottom walls. From the simulation, we find that the y-velocity profile is approximately parabolic, (see dotted curves in Figure 4 (a) and (b)) except above the pattern interface (where + or – zeta potentials meets). It is also found that y velocity is independent of x or z velocity components. The parabolic y-velocity's magnitude becomes zero at the interface, and changes sign as it crosses the interface. This transition occurs slowly as the particle travels along the channel, from cross-section 1 to 2 in Figure 3. As we track particles q and r in Figure 3, their z-position changes as they travel along the channel. The change in magnitude and direction of their y-velocity, as well as their z-position, are summarized in Figure 4 (a)-(d). At cross-section 1, particle q moves to the right at peak speed, while particle r moves rather slowly (Figure 4 (a)). As the particles move along the channel, the parabolic velocity profile changes direction, as well as the z-position of particles q and r. Now, the particle r moves towards the left at full speed, while particle q does the same at reduced speed. After passing a stripe, the net motion of particles q and r can be summarized as shown in Figure 4 (c). This net motion produces the net vortex shown in Figure 4 (d).

Using this secondary vortex as a building block, we can mimic the blinking vortex concept as the fluid travels along the channel. The blinking vortex is used for the microchannel by Stroock et al.[10] for pressure-driven flow. In electro-osmotic flow, one can also produce a blinking vortex using a pattern as shown in Figure 2 (b). The pattern consists of sloped coatings where one side is longer than the other. This unequal length coating is repeated for at least 5 stripes along the channel length direction to produce effective mixing. The pattern stirs the fluid as shown in Figure 7 (a), and is followed by another slightly different pattern, which produces the stirring as shown in Figure 7 (b).

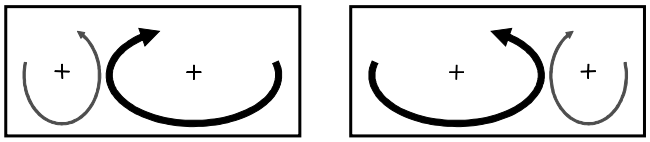

(a) ½ cycle (b) next ½ cycle

Figure 5: Mixing from herringbone pattern (*x* plane view)

Through numerical simulation the mechanism of secondary vortex and blinking vortices are successfully reproduced. These results are discussed later in this paper.

NUMERICAL FORMULATION

In a straight microchannel with insulated side walls, the electric potential gradient is constant along the channel if the external electric field is assumed to be unaffected by the zeta potential variation. Hence the solution of Laplace's equation is not needed to determine the external electric potential gradient. One can simply determine the wall boundary conditions from the zeta potential and solve the fluid flow using a standard CFD solver, without any special modifications for the solution of the external electric potential. Because the channel cross-section dimensions are in the order of 10-100 microns, we can use the Helmholtz-Smoluchowski slip velocity boundary conditions for the simulation of electro-osmotic force near the wall. In our study of micromixer performance, flow simulations are conducted using Fluent (a commercial CFD package) at Reynolds number well below 0.1 to ensure that inertial effects are negligible; the flow is then close to the Stokes flow regime and can be considered to be independent of the Reynolds number.

At the patterned surface, the sudden change of wall velocities at the pattern interfaces may introduce singularities in velocity gradient and vorticity as the grid becomes is refined. However, the effect is limited to the local control volumes very close to the interface, and its influence does not propagate elsewhere into the flow. This fact has been verified through mesh independence tests, both spatially and temporally. The mass is also conserved even for the control volumes near the singularities.

A numerical study of mixing by solving for species concentrations using either Eulerian or Lagrangian simulations is computationally prohibitive at the large Péclet numbers of interest. Here an alternate method is used where hypothetical neutrally-buoyant tracer particles are injected upstream in the flow and their trajectories are computed. Since no random noise is added to the velocity field, this corresponds to a simulation at infinite Péclet number. In order to estimate the effect of high but finite Péclet numbers, a novel scheme is proposed that allows numerical results to be compared with experimental results at the same Péclet numbers. The effect of diffusion is modeled by averaging at any desired cross-section of the channel, once particle trajectories have been computed. We now describe this method in detail.

First, particles are tracked until they reach a desired location with their initial position tagged. We assume that the mean particle travel time to reach the channel exit is $t = L_{channel} / v_{ave}$, where Lchannel is the channel length and vave a measure of the average horizontal velocity in the channel. We define a diffusive length scale ΔW as

$$\Delta W = \sqrt{D_{AB} t} = \sqrt{\frac{D_{AB} L_{channel}}{v_{ave}}} = \frac{L_{channel}}{\sqrt{Pe \cdot R}}, \quad (1)$$

$$\frac{\Delta W}{L_{channel}} = \frac{1}{\sqrt{Pe \cdot R}}, \quad (2)$$

where R is the ratio of the length of the channel to its width. Using the diffusion length scale ΔW obtained above, the channel cross-section is divided into squares with side dimension equal to ΔW.

If we are mixing two fluids with initial concentration $C_A = 1$ and $C_B = 0$ respectively, the concentration within any square at the outlet cross-section can be estimated from the weighted average of the particles with concentration C_A and C_B, assuming they have been mixed by diffusion within a square of side ΔW. This provides the concentration distribution at the outlet from the following equation:

$$C_{A+B} = \frac{\#\text{of } C_A \text{ particles}}{\#\text{of } C_A \text{ particles} + \#\text{of } C_B \text{ particles}}. \quad (3)$$

For example, consider the square cell at the bottom right corner of the channel in Figure 6 (c): it contains a total of nine particles, with four black and five white. White particles are assigned a concentration value of 1 and black particles are assigned a concentration value of 0. Then the resulting concentration of the cell can be calculated as 5 / 9 = 0.556. These values of the concentration field within each cell can be used to calculate the average and standard deviation of the concentration for a given outlet cross-section area. This approximation assumes that the diffusion occurs only within a given cell, and not between them; that diffusion begins at the channel inlet; and that the approximate time-of-residence within the channel is given by $t = L_{channel} / v_{ave}$. Additionally, a large number of particles should be used in order to minimize statistical fluctuations. The number of particles needed is proportional to the Péclet number.

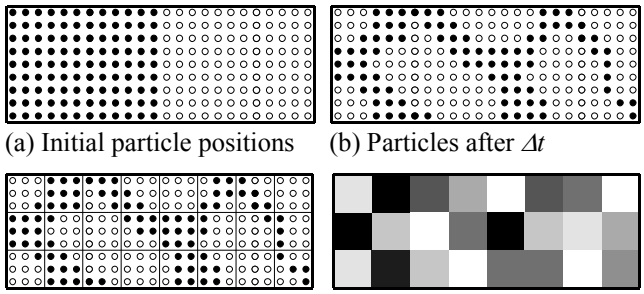

(a) Initial particle positions (b) Particles after Δt

(c) Division by ΔW (d) C_{A+B} from eq (3)

Figure 6: Estimation of standard deviation (*x* plane view)

RESULTS

Three-dimensional flow simulations for the pattern in Figure 2 (a) with different zeta potential combinations are performed. Our observation suggests that this combination of opposite zeta potentials yields very good stirring as well as relatively low mass flow reduction. With opposite zeta potential combinations, flow simulation is performed for 30 stripe pairs and particle track records at y-z cross-sections are shown in Figure 2. Each figure is taken after passing 5, 10, 15, and 30 stripe pairs. Significant mixing is achieved after 10 stripe pairs, forming a well-mixed arc-shaped region in the middle of the y-z cross-section. However, as the flow progresses through additional stripe pairs, no significant improvement in mixing is observed in the vicinity of the top channel surfaces. The bottom center contains an elliptic region that does not disperse into other part of the channel.

This lack of mixing can be eliminated using the concept of a blinking vortex [3] as discussed earlier, where we introduced two asymmetrically-placed vortices instead of one centered vortex. These are oriented along the net flow direction, and their strength varies periodically with a dominant vortex on one side associated with a weaker vortex on the other side. The top view of the pattern is shown in Figure 2 (b). The shaded portion will have opposite zeta potential with respect to the rest of the channel surface, thus providing strong resistance against the nearby flow. The particle paths are calculated at the end of each half cycle. Numerical results for the concentration field at ½, 1, 1½, and 6 cycles are presented in Figure 8. These results are generated using the procedure described in the previous section, with 15,000 particles. The Reynolds number for the calculation is 0.14. With this flow data, a micro-channel with cross-section dimensions of 200 × 33 μm and a length of each cycle of 3.5 mm is examined. The Péclet number is varied from 20,000 to 400,000, corresponding to diffusive mixing channel lengths of 4 μm to 80 μm.

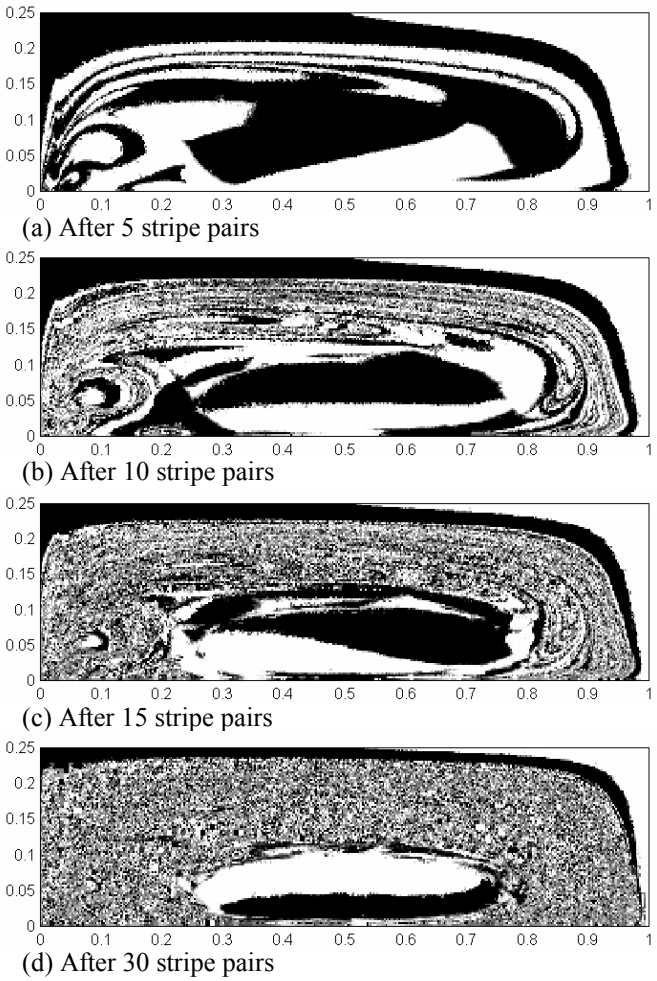

(a) After 5 stripe pairs

(b) After 10 stripe pairs

(c) After 15 stripe pairs

(d) After 30 stripe pairs

Figure 7: Mixing using the straight pattern (*x* plane view)

Using equation (3), the standard deviation (mean vs. concentration of each cell) is calculated at the end of each cycle, and its natural logarithm is plotted in Figure 9 with and without mixer. We offer some comments: (i) There is a tremendous increase in mixing efficiency, which is a direct consequence of the herringbone patterns; (ii) The decay of the standard deviation is roughly exponential in the length; (iii) the rate of exponential decay with length is approximately independent of the Péclet number. These three features are expected of chaotic mixing [2], and together offer compelling evidence that the micromixer is operating in the chaotic regime. The asymptotic rate is approximately equal to $0.11 mm^{-1}$, as indicated by the dashed line in Figure 9. This means that the mixer length required to decrease the standard deviation by half is about 6.3 mm.

Note that a constant value has been subtracted from each curve in Figure 9, because the standard deviation is not decaying to zero. Even though the herringbone pattern eliminates the most important elliptic island in the bottom-center of the channel, there remain isolated regions of poorly-

mixed regions, especially at the edges of the mixer, as can be seen in Figure 8. The nonzero asymptotic value for the standard deviation reflects solute caught in these regions and diffusing at the slow molecular rate. A different asymptotic value is used for each Péclet number, because the gridding procedure used to calculate the standard deviation resolves smaller unmixed regions as the Péclet number increases.

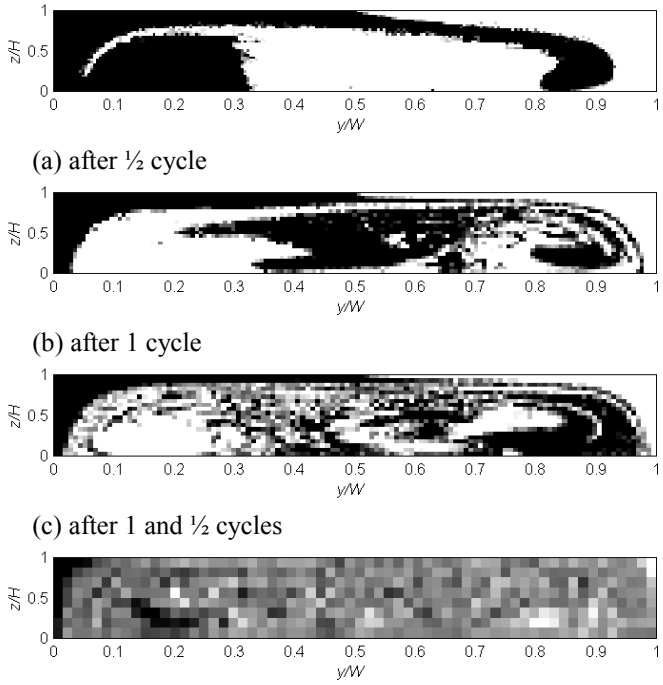

(a) after ½ cycle

(b) after 1 cycle

(c) after 1 and ½ cycles

(d) after 6 cycles

Figure 8: Mixing using the herringbone pattern (*x* plane view)

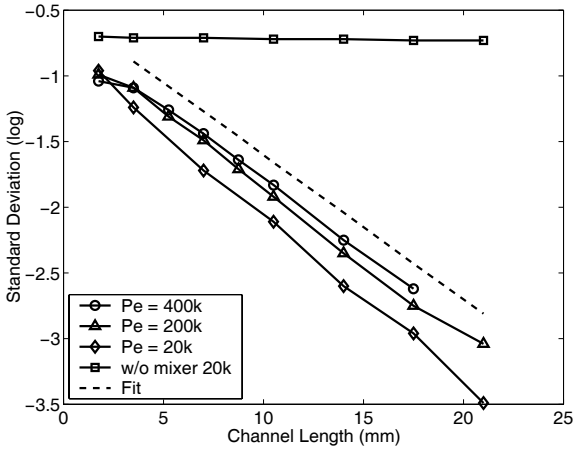

Figure 9: Logarithm of the standard deviation calculated for the herringbone pattern.

DISCUSSION

Using numerical simulations, we have demonstrated the feasibility of a micromixer that can work in the Stokes flow regime. With periodic zeta potential patterns, it is possible to generate a vortex that is aligned with the net flow direction. Straight striped zeta potential patterns produce a single vortex, with an elliptic region (unmixed island) and a chaotic mixing region that surrounds the island. Using a herringbone pattern, a mixing scheme similar to the blinking vortex can be generated, and this improves mixing by breaking up the unmixed elliptic island. The proposed mixing scheme can be implemented easily without the need for a multi-layer microfabrication process or moving parts, and can be operated without the need for extra power source (e.g., extra electric field) which many active mixers require [7,9,12]. Further optimization of the surface pattern will make the channel length shorter and mixing time smaller. Using the proposed mixing mechanism, an efficient micromixer can be designed and incorporated into the μTAS chip.

ACKNOWLEDGMENTS

Partial support for this work was provided by the National Science Foundation through award ECS 99-80828. The authors gratefully acknowledge this support.

REFERENCES

1. A. Ajdari, “Electro-Osmosis on Inhomogeneously Charged Surfaces”, Physical Review Letters **75**, 755-758 (1995)
2. T.M. Antonsen, Jr., Z. Fan, E. Ott, E. Garcia-Lopez. “The Role of Chaotic Orbits in the Determination of Power Spectra of Passive Scalars”, Physics of Fluids **8**, 3094-3104 (1996)
3. H. Aref, “Stirring by Chaotic Advection”, Journal of Fluid Mechanics **143**, 1-21 (1984)
4. E. B. Cummings, S. K. Griffiths, R.H. Nilson, “Irrotationality of Uniform Electro-osmosis”, SPIE conference on Microfluidic Devices and Systems II, Santa Clara, CA, 180-189 (1999)
5. J. Deval, P. Tabeling, C-M Ho, “A Dielectro-phoretic Chaotic Mixer”, Proceedings of the 15th IEEE International Conference on Micro Electro Mechanical Systems 2002, Las Vegas, NV, 36-39 (2002)
6. T.J. Johnson, D. Ross, L.E. Locascio, “Rapid Microfluidic Mixing”, Analytical Chemistry **74**, 45-51 (2002)
7. Y.-K. Lee, J. Deval, P. Tabeling, C.-M Ho, “Chaotic mixing in electrokinetically and pressure driven micro flows”, Proceedings of the 14th IEEE International Conference on Micro Electro Mechanical Systems 2001, 483-486 (2001)
8. R. H. Liu, M. A. Stremler, K. V. Sharp, M. G. Olsen, J. G. Santiago, R.J. Adrian, H. Aref, D.J. Beebe, “Passive mixing in a 3D serpentine microchannel”, Journal of Microelectromechanical Systems **9**, 190-197 (2000)
9. M. H. Oddy, J. G. Santiago, and J. C. Mikkelsen, "Electrokinetic Instability Micromixing," Analytical Chemistry **73**, 5822-5832 (2001)
10. A. D. Stroock, S. K. W. Dertinger, A. Ajdari, I. Mezic, H. A. Stone, G. M. Whitesides, “Chaotic Mixer for Microchannels”, Science **295**, 647-651 (2002)
11. A.D. Stroock, M.Weck, D.T. Chiu, W.T.S. Huck, P.J.A. Kenis, R.F. Ismagilov, G.M. Whitesides, “Patterning Electro-osmotic Flow with Patterned Surface Charge”, Physical Review Letters **84**, 3314-3317 (2000)
12. H. Suzuki, C-M Ho, “A Magnetic Force Driven Chaotic Micro-Mixer”, Proceedings of the 15th IEEE International Conference on Micro Electro Mechanical Systems 2002, Las Vegas, NV, 40-43 (2002)

